

# Traffic is a major source of atmospheric nanocluster aerosol

Topi Rönkkö<sup>1</sup>, Heino Kuuluvainen<sup>1</sup>, Panu Karjalainen<sup>1</sup>, Jorma Keskinen<sup>1</sup>, Risto Hillamo<sup>2</sup>, Jarkko Niemi<sup>3</sup>, Liisa Pirjola<sup>4</sup>, Hilikka Timonen<sup>2</sup>, Sanna Saarikoski<sup>2</sup>, Erkka Saukko<sup>1</sup>, Anssi Järvinen<sup>1</sup>, Henna Silvennoinen<sup>1</sup>, Antti Rostedt<sup>1</sup>, Miska Olin<sup>1</sup>, Jaakko Yli-Ojanperä<sup>1</sup>, Pekka Nousiainen<sup>5</sup>, Anu Kousa<sup>3</sup>, Miikka Dal Maso<sup>1</sup>

<sup>1</sup>Tampere University of Technology, <sup>2</sup>Finnish Meteorological Institute, <sup>3</sup>Helsinki Region Environmental Services Authority, <sup>4</sup>Metropolia University of Applied Sciences, <sup>5</sup>Turku University of Applied Sciences

Submitted to Proceedings of the National Academy of Sciences of the United States of America

In densely populated areas, traffic is a significant source of atmospheric aerosol particles. Due to their small size and complicated chemical and physical characteristics, atmospheric particles resulting from traffic emissions pose a significant risk for human health and but also contribute to anthropogenic forcing of climate. Previous research has established that vehicles directly emit primary aerosol particles but also contribute to secondary aerosol particle formation by emitting aerosol precursors. Here, we extend the urban atmospheric aerosol characterization to cover nanocluster aerosol (NCA) and show that a major fraction of particles emitted by road transportation are in a previously unmeasured particle size range of 1.3-3.0 nm. For instance, in a semi-urban roadside environment, the NCA represented 20% - 54% of the total particle number concentration of ambient air. The observed NCA concentrations varied significantly depending on the traffic rate and wind direction. The number emission factors of NCA for traffic were  $2.4 \cdot 10^{15} \text{ (kg}_{\text{fuel}})^{-1}$  in a roadside environment,  $2.6 \cdot 10^{15} \text{ (kg}_{\text{fuel}})^{-1}$  in a street canyon, and  $2.9 \cdot 10^{15} \text{ (kg}_{\text{fuel}})^{-1}$  in an on-road study through Europe. Interestingly, the emission was not associated with all vehicles. In engine laboratory experiments, the emission factor of exhaust NCA varied from a relatively low value,  $1.6 \cdot 10^{12} \text{ (kg}_{\text{fuel}})^{-1}$ , to a high value of  $4.3 \cdot 10^{15} \text{ (kg}_{\text{fuel}})^{-1}$ . The newly discovered NCA emissions directly affect particle concentrations and human exposure on nano-sized aerosol in urban areas and they may potentially act as nano-sized condensation nuclei for the condensation of atmospheric low-volatile organic compounds.

nanocluster aerosol | atmospheric aerosol | combustion-derived nanoparticles | air pollution | traffic emission

## Introduction

Detailed characterization of aerosol sources is required to understand climate impacts and health effects of atmospheric aerosols, as well as to develop technologies and policies capable of mitigating air pollution in urbanized areas. In densely populated areas one of the most significant source of particles is traffic.<sup>1,2</sup> Due to their small size and complicated chemical and physical characteristics<sup>3-6</sup>, atmospheric particles resulting from traffic emissions pose a significant risk for human health<sup>7-12</sup> and also contribute to anthropogenic forcing of climate<sup>13-14</sup>. Prior research on vehicular emissions has shown the existence of soot and ash<sup>3,15</sup> and solid sub-10 nm core particles<sup>4-6</sup> in primary emissions of vehicles and engines and their variation depending on vehicle technologies<sup>4,6</sup>, the properties of fuel and lubricant oil<sup>15,16</sup>, and driving conditions<sup>15-17</sup>. In addition to particles, exhaust typically contains species that reside in the gaseous phase in the undiluted high temperature exhaust<sup>5,17,18</sup>, but condense or even nucleate to the particle phase immediately after the exhaust is released to the atmosphere. Such aerosol is here called delayed primary aerosol, because particles' precursors exist already in the undiluted exhaust and the amount and characteristics of the resulting atmospheric particulate matter does not depend significantly on atmospheric processing or atmospheric photochemistry. In the

secondary aerosol formation process driven by atmospheric photochemistry, volatile gaseous compounds emitted by traffic are chemically transformed in the atmosphere to less volatile species enabling and enhancing secondary aerosol particle formation via condensation and new particle formation<sup>e.g.,20-22</sup>. While the primary and delayed primary particle emissions mostly affect the air quality near the emission source, the effect of the secondary processes is more important on a regional scale.

Previous research has shown the importance of nano-sized clusters in atmospheric processes, especially in the formation of ultrafine particles.<sup>23,24</sup> A number of studies also indicate that nano-sized clusters have a role in engine emission formation.<sup>4,25</sup> Preceding research of particle number concentrations near traffic has shown highly elevated concentrations (of the order of  $10^5$ - $10^6$ ) of ultrafine particles near roadways<sup>2,26</sup>, also indicating the likelihood of high concentrations of nano-sized particles and clusters existing in such environments. However, until now the measurement techniques suitable for their detection have not been applied in such environments, leaving the direct observation, formation, and effects of particles smaller than 3 nm still open.

Here, we report the significant presence nanocluster aerosol (NCA) particles in a particle diameter range of 1.3-3.0 nm of urban air. Our study strongly indicates that the source of this NCA is traffic, and more specifically, the exhaust of vehicles. We also show that the significance of NCA in vehicular emissions has been

## Significance

**We report the significant presence of traffic-originated nanocluster aerosol (NCA) particles in a particle diameter range of 1.3-3.0 nm of urban air, determine the emission factors for the NCA, and evaluate its global importance. Our finding is important because it significantly updates the current understanding of atmospheric aerosol in urban areas: the study shows that in urban air, extremely small particles form a significant fraction of the total particle number and are a direct result of anthropogenic emissions, i.e., the emissions from road traffic. Thus it also implies that in urban areas no atmospheric nucleation process is necessary to form a large number of particles, which affect population health and climate.**

## Reserved for Publication Footnotes

137  
138  
139  
140  
141  
142  
143  
144  
145  
146  
147  
148  
149  
150  
151  
152  
153  
154  
155  
156  
157  
158  
159  
160  
161  
162  
163  
164  
165  
166  
167  
168  
169  
170  
171  
172  
173  
174  
175  
176  
177  
178  
179  
180  
181  
182  
183  
184  
185  
186  
187  
188  
189  
190  
191  
192  
193  
194  
195  
196  
197  
198  
199  
200  
201  
202  
203  
204

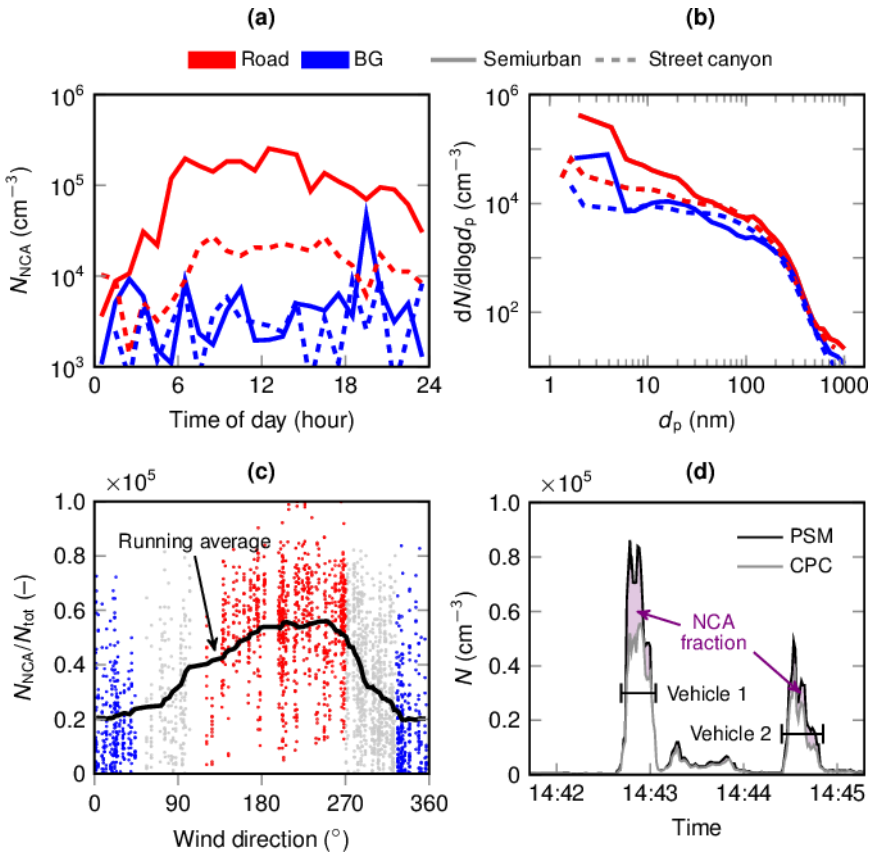


Fig. 1. Nanocluster aerosol (NCA) number concentrations in two different roadside environments, semi-urban (solid line, speed limit 80 km/h) and street canyon (dashed line, speed limit 40 km/h). (a) The diurnal variation of the NCA concentration. Two sectors, road (red, N=926) and urban background (blue, N=548) are distinguished from the data set based on the wind direction. (b) Particle number size distributions including the NCA of fresh exhaust aerosol measured in the roadside environments showing the high contribution of nanoclusters in total particle number. The road-influenced average distribution (red) and the average distribution from the clean sector (blue) representing the urban background are seen. (c) The ratio of NCA number concentration to the total aerosol number concentration as a function of the wind direction in the semi-urban environment. The nearest road is between the angles 110 – 270°. (d) An example of the time series measured with the PSM and a CPC, showing the effect of two passing vehicles on the particle concentration in the street canyon.

205  
206  
207  
208  
209  
210  
211  
212  
213  
214  
215  
216  
217  
218  
219  
220  
221  
222  
223  
224  
225  
226  
227  
228  
229  
230  
231  
232  
233  
234  
235  
236  
237  
238  
239  
240  
241  
242  
243  
244  
245  
246  
247  
248  
249  
250  
251  
252  
253  
254  
255  
256  
257  
258  
259  
260  
261  
262  
263  
264  
265  
266  
267  
268  
269  
270  
271  
272

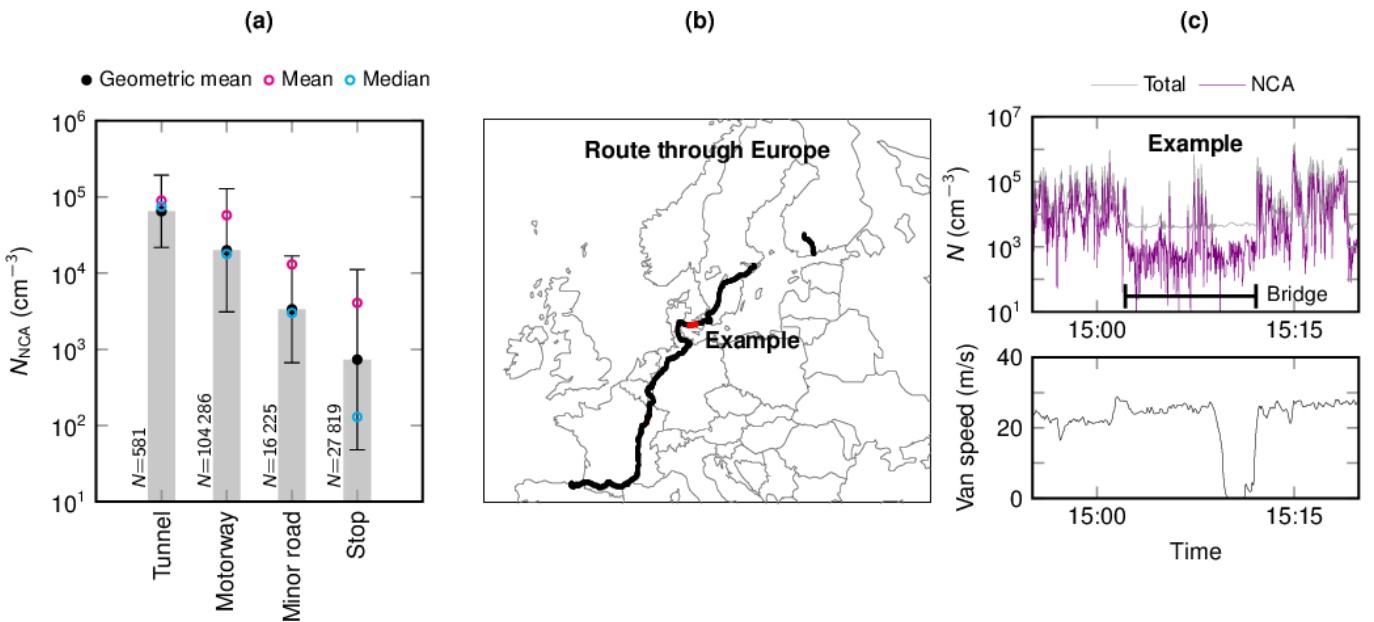
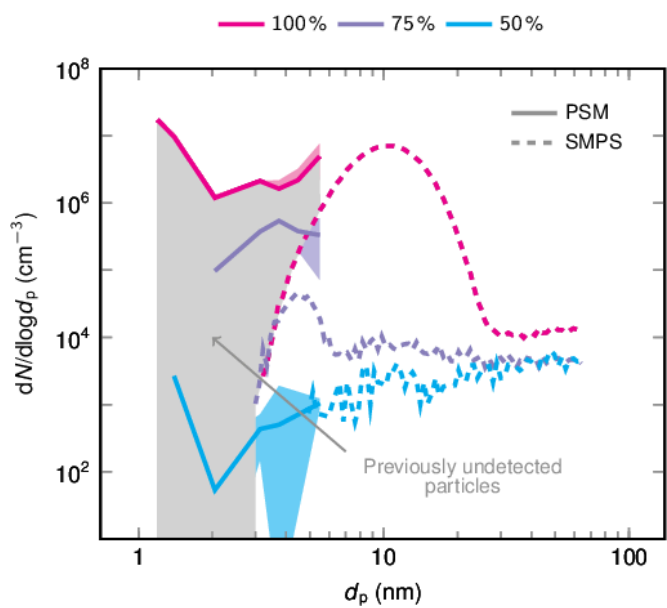


Fig. 2. Nanocluster (NCA) concentrations measured during the on-road experiment. In (a), geometric means, means and medians of NCA concentrations are shown in different experimental situations. In (b), the whole studied route is indicated by black line, location of measurements shown in (c) is indicated by red color. In (c), an excerpt of NCA and total particle concentration time series and speed profile of the mobile laboratory van is shown. Longer time series for the experiment are shown in Supporting Information.

previously underestimated due to a lack of knowledge and suitable measurement techniques. The observations reported here are based on the results from three atmospheric measurements covering a wide range of environments: stationary measurements at the roadside of a main road in a semiurban area, stationary

measurements in a street canyon in an urban area, and a long-distance on-road study by a mobile aerosol laboratory. Further evidence for the existence of the NCA in traffic emissions was obtained in a laboratory study in which emissions of a modern diesel engine were characterized. The NCA measurements were

273  
274  
275  
276  
277  
278  
279  
280  
281  
282  
283  
284  
285  
286  
287  
288  
289  
290  
291  
292  
293  
294  
295  
296  
297  
298  
299  
300  
301  
302  
303  
304  
305  
306  
307  
308  
309  
310  
311  
312  
313  
314  
315  
316  
317  
318  
319  
320  
321  
322  
323  
324  
325  
326  
327  
328  
329  
330  
331  
332  
333  
334  
335  
336  
337  
338  
339  
340



**Fig. 3.** Particle number size distributions of fresh exhaust aerosol measured in an engine laboratory, showing the high contribution of nanoclusters in total particle number for a diesel engine with three engine loads (50%, 75%, and 100%). The previously undetected particles are shadowed by gray color. The PSM (particle size magnifier, solid lines) and the SMPS (scanning mobility particle sizer, dashed lines) were used after the exhaust sampling and dilution system designed to mimic real-world nanoparticle formation. The shadowed areas represent the error limits for the PSM measurements formed by the standard deviations.

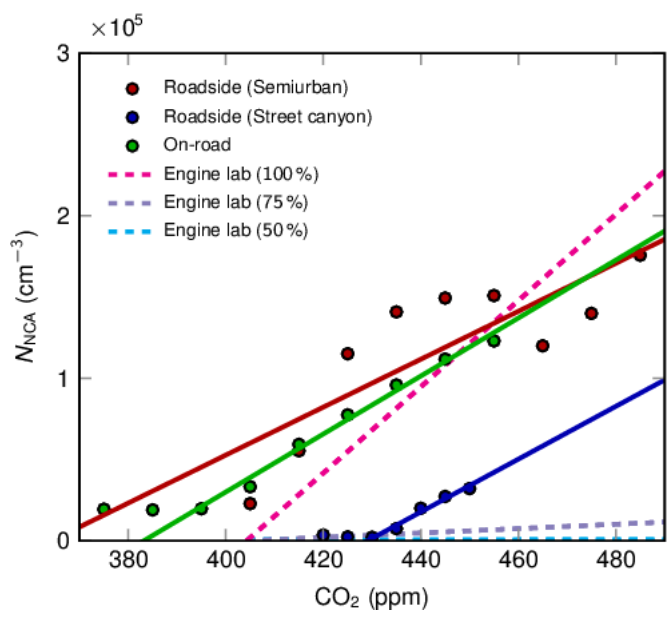


**Fig. 4.** The NCA number concentration as a function of simultaneously measured  $\text{CO}_2$ . Both roadside measurements, high-speed motorway driving during long-range on-road study through Europe and engine laboratory experiments are shown. The dots represent the experimental data averaged over discrete  $\text{CO}_2$  levels. In the cases of roadside and on-road studies, the solid lines are fits for the experimental data while the dashed lines for engine laboratory results are generated based on the NCA concentration measured at by one well-defined dilution stage.

performed using a Particle Size Magnifier (PSM)<sup>27</sup> which uses the method for NCA detection suggested by Iida et al.<sup>28</sup> and enables

the detection of extremely small nanoparticles. The method is currently generally adopted in nanoparticle formation studies<sup>24</sup>.

**Results and discussion**

In traffic environments, high NCA concentrations were observed when the wind was blowing from the road to the measurement site. Figure 1a shows the average diurnal variation of NCA concentrations measured in a semi-urban roadside location (solid lines) and in a street canyon (dashed lines). The concentrations are given separately for two prevailing wind sectors: “BG” refers to the situations where the wind was blowing from the urban background area towards the monitoring station, whereas “Road” refers to the situation where the wind direction was from the street or road towards the monitoring station. Data for all wind directions can be found in the Supporting Material (Fig. S9). In general, when the wind was blowing from the road towards the monitoring station, the NCA concentrations reached values higher than  $10^5 \text{ cm}^{-3}$  in the semi-urban environment and  $10^4 \text{ cm}^{-3}$  in the street canyon environment. The diurnal variation of the NCA number concentration was similar in both measurements; the NCA concentration increased rapidly at early morning and decreased to very low values in the evening.

The particle size distribution analysis (Fig. 1b) indicates that in the semi-urban roadside environment the observed NCA formed a separate mode with high number concentrations. However, a clearly distinguishable NCA mode was not observed in the street canyon. Naturally, also the loading of particles larger than 3 nm was higher in the road-originated air: in the semiurban roadside environment the median number concentration was  $1.3 \cdot 10^5 \text{ cm}^{-3}$ , compared to  $7.6 \cdot 10^4 \text{ cm}^{-3}$  for the background sector. Like the NCA concentrations, -the fraction of NCA in the total particle concentration also depended on the wind direction. In the semiurban roadside environment, on average 38% of measured aerosol particles in number belonged to NCA, i.e., to the size range from 1.3 to 3 nm. When the wind direction was from the road to the monitoring station, the NCA fraction increased to  $54 \pm 18\%$  ( $N = 926$ ). This value is the mean of the red dots shown in Fig. 1c, each of which corresponds to a 5 min. average of the measured concentrations. The standard deviation and the number of data points ( $N$ ) are also shown. In the background aerosol, the NCA fraction was lower, averaging  $20 \pm 17\%$  ( $N = 548$ ). Based on this evidence (diurnal variation and the effect of wind direction on the NCA concentration and fraction) we conclude that road traffic is a major source of NCA. Interestingly, not all vehicles emit high amounts of NCA. This is demonstrated by Fig. 1d which shows the concentration time series measured with a PSM and a condensation particle counter (CPC). The NCA concentration is obtained as the concentration difference of the two readings, and one can see that the passing of vehicle 1 resulted in a high amount of NCA (approximately 30% of the total concentration), whereas after vehicle 2, a much lower fraction of NCA was observed.

For a more regional evaluation, we conducted an on-road NCA experiment across Western Europe, from northern Spain to Finland (Fig. 2b). The experiment was mostly conducted on motorways (71% of all en-route observations) using a mobile laboratory equipped with similar instrumentation for the measurement of NCA as in the previous roadside studies. The NCA concentrations were particularly elevated in high-speed traffic environments, and lower when traffic influence was reduced, e.g., during stoppages and on minor roads (Fig 2a). The traffic influence is clearly demonstrated during the bridge crossing the Danish Straits (Fig 2c). The crossing was performed during heavy cross-wind conditions, which in practice caused the instruments to sample only marine background. At this time, both the concentration and fraction of NCA was drastically reduced. On-road observations also showed that different road environments

341  
342  
343  
344  
345  
346  
347  
348  
349  
350  
351  
352  
353  
354  
355  
356  
357  
358  
359  
360  
361  
362  
363  
364  
365  
366  
367  
368  
369  
370  
371  
372  
373  
374  
375  
376  
377  
378  
379  
380  
381  
382  
383  
384  
385  
386  
387  
388  
389  
390  
391  
392  
393  
394  
395  
396  
397  
398  
399  
400  
401  
402  
403  
404  
405  
406  
407  
408

409 result in different NCA loadings (Fig. 2a) – high-speed motorways  
410 exhibited higher NCA concentration than minor roads with lower  
411 speeds, and the highest NCA concentrations were measured in  
412 traffic tunnels where the dilution of exhaust emissions is limited.

413 The observations presented above strongly indicate that NCA  
414 observed in urban and traffic environments is emitted by traffic  
415 rather than from atmospheric particle formation. To gain evi-  
416 dence of NCA as a byproduct of combustion, we performed three  
417 laboratory experiments with a modern diesel engine. We observed  
418 that, in addition to soot and nucleation mode particles larger than  
419 3 nm, the exhaust contained a significant amount of NCA (Fig. 3).  
420 The NCA concentration depended on the engine load in a similar  
421 way than the concentration of particles in the size range above 3  
422 nm. It should be noted that in the engine laboratory experiment  
423 the exhaust dilution and sampling system enables real-world-  
424 like nanoparticle formation<sup>29</sup> but does not emulate atmospheric  
425 oxidation. As discussed previously, secondary aerosol formation  
426 requires that gaseous emissions are oxidized to low-volatility  
427 compounds. Our experiments show that fresh exhaust can con-  
428 tain sufficient low volatility compounds that NCA formation in  
429 vehicle exhaust is possible without atmospheric oxidation. We  
430 also observed that, by using thermal treatment for the exhaust  
431 sample, the NCA disappeared at 75% engine load and nearly  
432 disappeared at 100% load (see Fig. S8). This indicates that the  
433 NCA should be considered to be delayed primary aerosol, and  
434 composed of species that were not in the particle phase in hot  
435 undiluted exhaust. However, the total NCA emission of traffic is  
436 a result of emissions from a large number of vehicles with varying  
437 technologies; this may cause significant variation the formation  
438 mechanism and composition of emitted NCA.

440 CO<sub>2</sub> is an inert gas and a product of combustion; it can,  
441 therefore, be used as a tracer for combustion-originated prod-  
442 ucts in the atmosphere, i.e., to determine fuel specific emission  
443 factors for other byproducts of combustion.<sup>30,31</sup> Furthermore,  
444 such emission factors enable the comparison of emissions from  
445 different combustion sources. Figure 4 shows the dependence of  
446 the NCA concentration on CO<sub>2</sub> for each experiment conducted  
447 in this study (two roadside experiments, the on-road study and  
448 three experiments in the engine laboratory). For the roadside  
449 and on-road experiments, the figure shows the measurement data  
450 averaged over discrete CO<sub>2</sub> levels (at intervals of 5 or 10 ppm),  
451 and linear fits for the averaged data points above the background  
452 CO<sub>2</sub> level (see also Supporting Information on the background  
453 CO<sub>2</sub> concentrations of ambient air). For the engine laboratory  
454 experiments, the figure shows lines measured at one phase of  
455 exhaust dilution and calculated into the larger dilution scene.

456 For the roadside experiment conducted in the street canyon  
457 and for the on-road experiment, the NCA concentration in-  
458 creased linearly as a function of CO<sub>2</sub> concentration when the  
459 CO<sub>2</sub> values were above the background value. In the semi-urban  
460 roadside experiment, the linear dependence was not as clear-cut.  
461 For all three cases, slopes of the fits were similar:  $1475 \pm 918$   
462  $(\text{cm}^3\text{ppm})^{-1}$  for the semiurban roadside environment,  $1625 \pm 1062$   
463  $(\text{cm}^3\text{ppm})^{-1}$  for the street canyon, and  $1784 \pm 309$   $(\text{cm}^3\text{ppm})^{-1}$   
464 for the high-speed motorway driving during the trans-European  
465 on-road study. Assuming a CO<sub>2</sub> emission of 3140 g/kg fuel (an  
466 average of conversion factors for diesel and gasoline fuels) and  
467 NTP,<sup>30</sup> we computed fuel specific number emission factors for  
468 the NCA:  $2.4 \cdot 10^{15} \pm 1.5 \cdot 10^{15} (\text{kg}_{\text{fuel}})^{-1}$ ,  $2.6 \cdot 10^{15} \pm 1.7 \cdot 10^{15} (\text{kg}_{\text{fuel}})^{-1}$   
469 and  $2.9 \cdot 10^{15} \pm 0.5 \cdot 10^{15} (\text{kg}_{\text{fuel}})^{-1}$  for the three environments, re-  
470 spectively. The error limits were formed from the 95% confidence  
471 limits obtained for the slopes of the fits (Fig. 4). For the engine  
472 laboratory experiments the fuel specific emission factors for NCA  
473 were  $1.6 \cdot 10^{12} (\text{kg}_{\text{fuel}})^{-1}$  at low load,  $2.2 \cdot 10^{14} (\text{kg}_{\text{fuel}})^{-1}$  at medium  
474 load and  $4.3 \cdot 10^{15} (\text{kg}_{\text{fuel}})^{-1}$  at high load (diesel fuel, thus assuming  
475 a CO<sub>2</sub> emission of 3160 g/kg fuel and NTP<sup>30</sup>). Thus, the traffic

477 NCA emissions determined in the three field experiments were  
478 between the minimum and maximum emission factors observed  
479 in the laboratory study. When compared to other studies,<sup>30,31</sup> it  
480 can be concluded that the NCA emission factors of traffic are  
481 at same level with the emission factors of larger particles. In  
482 the worldwide perspective, the annual NCA emissions of road  
483 traffic are likely to exceed  $4.2 \cdot 10^{27}$  per year (see Supporting In-  
484 formation), which represents a significant increase to the existing  
485 estimate of  $17 \cdot 10^{27} \text{ a}^{-1}$  for global anthropogenic particle sources<sup>32</sup>.

486 Recent studies<sup>33</sup> have shown strong indications that a large  
487 fraction of secondary organic aerosol (SOA) formation is due to  
488 extremely low volatility vapors condensing on available aerosol  
489 surfaces. We show here that traffic-emitted NCA increases the  
490 aerosol particle number concentrations in environments near  
491 traffic. Prior research has shown that particle concentrations  
492 decrease when moving away from the roadway; this is generally  
493 attributed to coagulation and dilution<sup>2,26,34</sup>, although also evapo-  
494 ration has been suggested<sup>35</sup>. The scavenging timescale of diluted  
495 NCA is of the order of 20 minutes to reach the levels observed for  
496 urban background aerosol. Therefore, NCA can be transported  
497 for several kilometers before removal by loss processes meaning  
498 that in urban areas the traffic-originated NCA is likely ubiquitous,  
499 and itself contributes significantly to the background. Comparing  
500 to other NCA sources, in urban environments traffic-emitted  
501 NCA is likely to exceed the number of particles formed by photo-  
502 chemical nucleation. High anthropogenic aerosol concentrations  
503 have typically been considered as an inhibiting factor in terrestrial  
504 boundary layer nucleation due to their effect in scavenging both  
505 condensing vapors and fresh nanoparticles from the air. Regional  
506 photochemical formation is considered to be the major source of  
507 NCA-sized aerosol in the atmosphere. Our finding updates this  
508 view, showing that human activity also directly produces nano-  
509 sized aerosol which may allow even a majority of the condensa-  
510 tional growth events of atmospheric aerosol particles to begin in  
511 urban areas, reported, e.g., by Ahlm et al.<sup>37</sup>, by acting as nano-  
512 sized condensation nuclei for both secondary anthropogenic and  
513 biogenic low-volatility organic compounds. Thus, the NCA has  
514 the potential to enhance tropospheric aerosol formation, and by  
515 that route, modify terrestrial cloud cover. Therefore, our find-  
516 ing opens new possibilities to understand atmospheric processes  
517 affecting climate, in addition to presenting a new anthropogenic  
518 NCA source that may affect urban air quality and therefore also  
519 public health.

## 521 Methods

522 **Atmospheric measurements.** The studies consisted of three atmospheric  
523 measurements covering a wide range of environments: stationary measure-  
524 ments at the roadside of a main road in a semi-urban area, stationary  
525 measurements in a street canyon in an urban area and a long-distance on-  
526 road study using a mobile aerosol laboratory. The nanocluster aerosol (NCA)  
527 measurements were performed using an instrument capable of detecting  
528 extremely small nanoparticles, with diameters of as small as ca. 1.3 nm  
529 (Particle Size Magnifier, PSM)<sup>28</sup>. NCA measurements were reinforced by  
530 measurements with other instruments.

531 The experiment which produced the first observation of NCA in an urban  
532 traffic environment was conducted in a roadside environment between Octo-  
533 ber 19th and 30th in 2012. The measurement station was located at a distance  
534 of 5 m from the pavement of the ring road Ring 1, which is one of the main  
535 roads in Helsinki (Fig. S1). Daily traffic rate on that road during workdays is  
536 approximately 70'000 vehicles, including both heavy-duty vehicles (8%) and  
537 passenger cars. Ambient temperature and relative humidity varied between  
538 -5 and +14°C and 43-93%, respectively, and were continuously measured  
539 at a weather station located in Pasila (Fig. S1). Weather parameters were  
540 temporarily measured with a mobile laboratory<sup>37</sup> next to the measurement  
541 station with a good correlation with the continuous measurements. The  
542 measurement station data was classified based on the wind direction data  
543 into two relevant sectors and the sectors between these (Fig. S1b). The road-  
544 influenced sector was defined as wind directions 110-270° and the clean  
545 sector as directions 325-55° (with 0° as north).

546 The aerosol sample was drawn into the measurement station from the  
547 roof of the station (height 3 m) and then led to the online aerosol instru-  
548 ments. The combination of a particle size magnifier (PSM A09, Airmodus  
549

Oy) and a condensation particle counter (CPC model 3775, TSI Inc.), referred simply as a PSM, measured the concentration of particles larger than 1.3 nm. It was used parallel with CPC (model 3776 TSI Inc.) that measured the number concentration of the particles larger than 3 nm in diameter. The particle size distribution was measured with a differential mobility particle sizer (DMPS) equipped with a Vienna type DMA (differential mobility analyzer) and a CPC (model 5.401 Grimm Ltd). The DMPS covered a size range from 6 nm to 1 µm. Also gaseous pollutants NO<sub>x</sub> (APNA-360, HORIBA) and CO<sub>2</sub> (Maihak Sidor, SICK) were monitored. CO<sub>2</sub> concentrations were used in the evaluation of the emission factors of NCA.

The time series of the number concentrations measured by the PSM and the CPC is shown in Fig. S2a. For the purpose of the further analysis and visualization, the data was averaged over a 5-minute time window. The concentration of the NCA, i.e., the particles from 1.3 nm to 3 nm, was defined as the difference of the concentrations measured by these two devices. The relative number concentration normalized by the total number concentration  $N_{tot}$  measured by the PSM and classified according to the road influenced and clean sectors is shown in Fig. S2b. As seen in Fig. S2a, both the PSM and the CPC measured rather high concentrations around 10<sup>6</sup> #/cm<sup>3</sup> at the maximum. The actual counting instruments, CPC model 3775 and the CPC model 3776, were concentration calibrated in the laboratory after the field campaign based on the Single Charged Aerosol Reference<sup>38</sup>. The calibration results were further applied in the data-analysis. Due to the material dependency of the lower detection limits of a diethylene glycol based PSM and of a butanol based CPC<sup>39</sup>, this study may slightly underestimate the NCA concentrations.

In a street canyon environment in an urban area, the NCA concentrations were measured for three months. The measurement station was located on the pavement along a relatively busy road which leads towards Helsinki City Centre (Fig. S1). The exact address of the measurement station is Mäkelänkatu 50. The site can be classified as an avenue canyon with the aspect ratio (height/width) of 0.4 (Fig. S3). The road has 6 lanes with two tramlines and rows of trees in the middle. In total, the width of the road is 42 m. The road is flanked by 4- and 5-floor buildings. The traffic rate on Mäkelänkatu is approximately 28'000 vehicles/workday of which heavy-duty vehicles account for 9 %. Measurements were conducted between April 7th and June 26th in 2015. The temperature and relative humidity measured at the station varied between 2.1-21 °C (avg 8.6 °C) and 18.9-92.9 % (avg 65.1%), respectively. Wind direction measurements were performed at the weather station located in Pasila with measurement height at 53 m above ground and 78 m above sea level (Fig. S1), representing thus the roof-top wind at the measurement site. The measurement station data was divided according to the wind direction into two sectors and the sectors between these as seen in Fig. S1c. In the case of perpendicular flow, the local wind within the cavity of the canyon was assumed to be contrary to the roof-top wind. Consequently, the road influenced sector was between the angles 165-285° and the clean sector between the angles 0-105° and 345-360°.

The particle sample was drawn from the roof of the station (height 4 m) and then conducted to the online aerosol instruments in the measurement station. The setup consisted of a combination of a particle size magnifier (PSM model A10, Airmodus Oy) and a condensation particle counter (CPC model A20, Airmodus Oy), referred simply as a PSM. A bridge diluter (DR 7.55) was used in the sampling line before the PSM. The PSM was set to measure the number concentrations in a step-mode with four different cut-off sizes: 1.2, 1.5, 1.8, and 2.7 nm. The measurement duration for one step was 60 s and hence one cycle took 4 min in total. The diurnal hourly averages were calculated separately for each step and the NCA concentrations were determined from the concentration difference of the first and the last step. Sub-3 nm measurement points for the particle number size distributions were determined similarly from the step-data. Particle size distribution for larger particles was measured with a DMPS equipped with a Vienna type DMA and a CPC (model A20, Airmodus Oy). The DMPS covered a size range from 6 to 800 nm.

The on-road NCA emissions were studied with a mobile laboratory unit while driving in traffic. The mobile laboratory consists of a large van equipped with sampling systems for both gaseous and particulate compounds, a compartment where the instruments can be installed, a desktop space for the operator to control the measurement and a power source to supply the instruments. In Fig. S4a a picture of the mobile unit is shown, and a measurement situation on road is shown in Fig. S4b. The measurement route, shown in Fig. 2b (main text), started eastwards from the Atlantic coast in northern Spain. It then turned towards north from the Mediterranean coast in southern France and continued through France, Luxembourg, Belgium, the Netherlands, Germany and Denmark to the large bridges over the Great Belt and the Sound. From there the route continued through southern Sweden towards a ferry connection to Finland. The total distance covered within 6

days was ca. 3600 km. While the route consisted mainly of larger motorways, smaller highways and city traffic were also included where the schedule allowed.

The aerosol sample for the instruments was taken in front of the van from the centerline, just above the windscreen. The sampling probe was bent downstream of the flow in order to prevent insects and rain droplets entering to the sample. The sample line continued to the instrument compartment with a residence time of < 1s, where the sample was divided via a bridge diluter (DR=42) to the CPC 3776 (TSI Inc) and the PSM consisting of a Particle Size Magnifier (PSM model A10, Airmodus Oy) and a model 3775 CPC (TSI Inc.). CPC model 3776 (TSI Inc) measured the total particle number concentration for particles larger than 3 nm, while the total number concentration of particles larger than ca. 1.3 nm were measured with the PSM. CO<sub>2</sub> concentration was measured using an IR photometric analyzer (SIDOR, Sick Maihak). The measured data from all these instruments (shown in Fig S5) was saved with one-second time resolution. A weather station (WeatherStation 200WX, Airmar Technology Corporation) provided information on the wind speed and direction, air temperature, barometric pressure, relative humidity, GPS location, vehicle speed and vehicle direction in the sampling point. A time series of the measured air temperature (T), relative humidity (RH), barometric pressure (p) and altitude are shown in Fig S6.

**Engine laboratory experiments.** Laboratory experiments with a modern four-cylinder turbo-charged common rail heavy duty diesel engine (displacement 4.4 dm<sup>3</sup>) equipped with an intermediary cooling system for the intake air, a diesel oxidation catalyst (DOC), a diesel particle filter (DPF) and a selective catalytic reduction system (SCR) were conducted to verify the traffic environment observations. The ultra-low sulfur diesel fuel (FSC < 10 ppm) was used. Thus, the technology level of the test engine corresponds to the typical modern (and even future) heavy duty diesel buses, trucks and working machines. Three experiments were conducted at an engine test bench, each at different engine loading. The driving parameters and regulated emissions of each experiment are shown in Table S1.

The measurement setup is shown in Fig. S7. To mimic real-world nanoparticle formation, an exhaust sampling system<sup>40</sup> that has been reported to mimic exhaust nucleation mode particle formation relatively well<sup>29,41</sup> was used. By using this sampling system, a part of exhaust was sampled directly from the tailpipe and, further, diluted immediately using a porous tube type primary diluter<sup>42</sup>, led through a residence time chamber with a residence time of 2.6 seconds and, finally, diluted by an ejector secondary dilution unit. In the primary diluter the dilution air temperature was kept at 30 °C and the dilution ratio, calculated from CO<sub>2</sub> data from undiluted and diluted exhaust, was kept at 12. The relative humidity for the pressurized and filtered dilution air was close to zero. After the secondary dilution unit, the exhaust aerosol was led into the aerosol instruments. Because of the high stability of the particle concentrations, the PSM was used in the scanning mode, thus providing information on both the number concentration and size distribution of particles smaller than 3 nm in diameter. In order to convert the cumulative number concentration measured by the PSM to particle size distributions, calibrations for different saturator flows of the PSM was used.<sup>25</sup> In addition to the PSM, exhaust particle number size distributions were measured using scanning mobility particle sizer (SMPS)<sup>43</sup> equipped with a DMA 3085 (TSI Inc.) and a CPC 3025 (TSI Inc.), called here as Nano-SMPS, an engine exhaust particle sizer (EEPS, TSI Inc.)<sup>44</sup> and an Electrical Low pressure Impactor (ELPI, Dekati Inc)<sup>45</sup>. The EEPS and the ELPI were used to monitor the stability of the larger particle emission during the experiment. Particle volatility was studied using a thermodenuder<sup>5</sup> in which the aerosol sample was first heated to 265 °C and, after that, led through the denuder part to collect the evaporated compounds to active charcoal.

The data presented in the current manuscript has been stored in the Finnish IDA (opencience.fi/ida) storage service. Once the manuscript has been accepted, the metadata of the dataset will be updated to reflect this, and made available in the ETSIN (opencience.fi/etsin) research data service with a permanent download link. The link will also be added to the TUT research data system TUTCRIS (<https://tutcris.tut.fi/portal/en/datasets/search.html>). The direct and permanent link to the data download will be provided in the final manuscript.

#### Acknowledgements

Authors acknowledge financial support from Tekes (the Finnish Funding Agency for Innovation), Academy of Finland (grant no. 259016, grant no. 293437) and Clean Ltd (MMEA project), Dinex Ecocat Oy, Neste Oil Oy, AGCO Power, Oy Nanol Technologies Ab, Anders Svens and Harri Portin (HSY) are acknowledged for their technical support work in roadside measurements.

vehicle exhausts. *Environ. Sci. Technol.*, 42:859-863.

5. Rönkkö T. et al. (2013) Effects of gaseous sulphuric acid on diesel exhaust nanoparticle formation and characteristics. *Environ. Sci. Technol.* 47:11882-11889.

6. Lähde T. et al. (2009) Heavy Duty Diesel Engine Exhaust Aerosol Particle and Ion Measurements. *Environ. Sci. Technol.* 43:163-168.

7. Maher B. et al. (2016) Magnetite pollution nanoparticle in the human brain. *Proc Natl Acad*

1. Pey J et al. (2009) Source apportionment of urban fine and ultra fine particle number concentration in a Western Mediterranean city. *Atmos. Environ.* 43:4407-4415.
2. Hu S, Fruin S, Kozawa K, Mara S, Paulson S, Winer A (2009) A wide area of air pollutant impact downwind of a freeway during pre-sunrise hours. *Atm. Env.*, 43:2541-2549.
3. Kittelson D (1998) Engines and nanoparticles: a review. *J. Aerosol Sci.* 29:575-588.
4. Sgro L et al. (2008) Measurements of nanoparticles of organic carbon and soot in flames and

681	<i>Sci USA</i> 113(22):10797-10801.	
682	8. Hoek G, Brunekreef B, Goldbohm S, Fischer P, van den Brandt, P (2002) Association between mortality and indicators of traffic-related air pollution in the Netherlands: a cohort study. <i>Lancet</i> 360:1203–1209.	750
683		751
684	9. Oberdörster, G., Oberdörster, E. & Oberdörster, J. (2005) Nanotoxicology: An emerging Discipline Evolving from Studies of Ultrafine Particles. <i>Environ Health Perspect</i> 113:823–839.	752
685		753
686	10. Alföldy B, Gieschaskiel B, Hofmann W, Drossinos Y (2009) Size-distribution dependent lung deposition of diesel exhaust particles. <i>J. Aerosol Sci.</i> 40:652-663.	754
687		755
688	11. Lelieveld J, Evans JS, Fnais M, Giannadaki D, Pozzer A (2015) The contribution of outdoor air pollution sources to premature mortality on a global scale. <i>Nature</i> 525:367-371.	756
689		757
690	12. McConnell R et al. (2006) Traffic, susceptibility, and childhood asthma. <i>Environ Health Perspect</i> 114:766-772.	758
691		759
692	13. Haywood J, Boucher O (2000) Estimates of the direct and indirect radiative forcing due to tropospheric aerosols: A review. <i>Rev. Geophys.</i> 38:513-543.	760
693		761
694	14. Bond T et al. (2013) Bounding the role of black carbon in the climate system: A scientific assessment. <i>Journal of Geophysical Research: Atmospheres</i> 118:5380-5552.	762
695		763
696	15. Maricq MM, Chase R, Xu N, Laing P (2002) The effects of the catalytic converter and fuel sulfur level on motor vehicle particulate matter emissions: Light duty diesel vehicles. <i>Environ. Sci. Technol.</i> 36:283-289.	764
697		765
698	16. Vaaraslahti K et al. (2005) Effect of lubricant on the formation of heavy-duty diesel exhaust nanoparticles. <i>Environ. Sci. Technol.</i> 39:8497-8504.	766
699		767
700	17. Rönkkö T et al. (2014) Vehicle engines produce exhaust nanoparticles even when not fueled. <i>Environ. Sci. Technol.</i> 48:2043–2050.	768
701		769
702	18. Shi J, Harrison R (1999) Investigation of ultrafine particle formation during diesel exhaust dilution. <i>Environ. Sci. Technol.</i> 33:3730-3736.	770
703		771
704	19. Arnold F et al. (2012) First online measurements of sulfuric acid gas in modern heavy-duty diesel engine exhaust: implications for nanoparticle formation. <i>Environ. Sci. Technol.</i> 46:11227–11234.	772
705		773
706	20. Robinson A et al. (2007) Rethinking organic aerosols: Semivolatile emissions and photochemical aging. <i>Science</i> 315:1259-1262.	774
707		775
708	21. Platt S et al. (2014) Two-stroke scooters are a dominant source of air pollution in many cities. <i>Nature Communications</i> 5:3749.	776
709		777
710	22. Gentner D et al. (2012) Elucidating secondary organic aerosol from diesel and gasoline vehicles through detailed characterization of organic carbon emissions. <i>Proc Natl Acad Sci USA</i> 109:18318-18323.	778
711		779
712	23. Kulmala M et al. (2007) Toward direct measurement of atmospheric nucleation. <i>Science</i> 318:89-92.	780
713		781
714	24. Lehtipalo K et al. (2016) Ion-induced nucleation of pure biogenic particles. <i>Nature</i> 533:521–526.	782
715		783
716	25. Alanen J et al. (2015) The formation and physical properties of the particle emissions from a natural gas engine. <i>Fuel</i> , 162:155-161.	784
717		785
718	26. Zhu Y, Hinds W, Kim S, Shen S, Sioutas C. (2002) Study of ultrafine particles near a major highway with heavy-duty diesel traffic. <i>Atm. Env.</i> 36: 4323-4335.	786
719		787
720	27. Iida K, Stolzenburg M, McMurry P (2009) Effect of working fluid on sub-2 nm particle detection with a laminar flow ultrafine condensation particle counter. <i>Aerosol Sci. Technol.</i> , 43:81-96.	788
721		789
722	28. Vanhanen J et al. (2011) Particle size magnifier for nano-CN detection. <i>Aerosol Sci. Technol.</i> 45:533-542.	790
723		791
724		792
725		793
726		794
727		795
728		796
729		797
730		798
731		799
732		800
733		801
734		802
735		803
736		804
737		805
738		806
739		807
740		808
741		809
742		810
743		811
744		812
745		813
746		814
747		815
748		816
	29. Keskinen J, Rönkkö T (2010) Can real-world diesel exhaust particle size distribution be reproduced in the laboratory? A critical review. <i>Journal of the Air &amp; Waste Management Association</i> 60:1245-1255.	
	30. Yli-Tuomi T et al. (2005) Emissions of the particles, NOx, and CO from on-road vehicles in Finland. <i>Atmos. Environ.</i> 39:6696-6706.	
	31. Pirjola L et al. (2016) Physical and chemical characterization of real-world particle number and mass emissions from city buses in Finland. <i>Environ. Sci. Technol.</i> 50:294-304.	
	32. Paasonen P et al. (2016) Continental anthropogenic primary particle number emissions. <i>Atmos. Chem. Phys.</i> 16:6823-6840.	
	33. Ehn M et al. (2014) A large source of low-volatility secondary organic aerosol. <i>Nature</i> 506:476-479.	
	34. Jacobson M, Seinfeld J (2004) Evolution of nanoparticle size and mixing state near the point of emission. <i>Atmos. Environ.</i> 38:1839-1850.	
	35. Zhang K, Wexler A, Zhu Y, Hinds W, Sioutas C (2004) Evolution of particle number distribution near roadways. Part II: The 'Road-to-Ambient' process. <i>Atmos. Environ.</i> 38:6655-6665.	
	36. Ahlm L et al. (2012) Formation and growth of ultrafine particles from secondary sources in Bakersfield, California. <i>Journal of Geophysical Research Atmospheres</i> 117 (5): D00V08.	
	37. Pirjola L et al. (2004) "Sniffer"—a novel tool for chasing vehicles and measuring traffic pollutants. <i>Atmos. Environ.</i> 38:3625-3635.	
	38. Yli-Ojanperä J, Mäkelä JM, Marjamäki M, Rostedt A, Keskinen J (2010) Towards traceable particle number concentration standard: Single charged aerosol reference (SCAR). <i>J. Aerosol Sci.</i> 41:719-728.	
	39. Kangasluoma J et al. (2014) Sub-3 nm particle size and composition dependent response of a nano-CPC battery. <i>Atmos. Meas. Tech.</i> 7:689–700.	
	40. Ntziachristos L et al. (2004) Performance evaluation of a novel sampling and measurement system for exhaust particle characterization. <i>SAE Technical Paper Series</i> 2004-01-1439.	
	41. Rönkkö T et al. (2006) Effect of dilution conditions and driving parameters on nucleation mode particles in diesel exhaust: Laboratory and on-road study. <i>Atmos. Environ.</i> 40:2893-2901.	
	42. Mikkonen P, Moision M, Keskinen J, Ristimäki J, Marjamäki M (2001) Sampling method for particle measurements of vehicle exhaust. <i>SAE Technical Paper Series</i> 2001-01-0219.	
	43. Wang S, Flagan R (1990) Scanning electrical mobility spectrometer. <i>Aerosol Sci. Technol.</i> 13:230-240 (1990).	
	44. Johnson T, Caldow R, Pöcher A, Mirme A, Kittelson D (2004) A new electrical mobility particle sizer spectrometer for engine exhaust particle measurements. <i>SAE Technical Paper Series</i> 2004-01-1341.	
	45. Keskinen J, Pietarinen K, Lehtimäki M (1992) Electrical low pressure impactor. <i>Journal of Aerosol Science</i> 23:353-360.	
	46. Fernández-Duque B, Pérez I, Sánchez M, García M, Pardo N (2017) Temporal patterns of CO2 and CH4 in a rural area in northern Spain described by a harmonic equation over 2010–2016. <i>Science of the Total Environment</i> 593-594: 1-9.	
	47. Wu J et al. (2012) Evolution of atmospheric carbon dioxide concentration at different temporal scales recorded in a tall forest (2012). <i>Atmos. Environ.</i> 61:9-14.	
	48. IEA website. CO2 emissions from fuel combustion highlights 2015. <a href="http://www.iea.org/publications/freepublications/publication/co2-emissions-from-fuel-combustion-highlights-2015.html">http://www.iea.org/publications/freepublications/publication/co2-emissions-from-fuel-combustion-highlights-2015.html</a> . Visited 14 <sup>th</sup> September, 2016.	